small NANO MICRO

Phospholipid patterns

Preparation of Phospholipid Multilayer Patterns of Controlled Size and Thickness by Capillary Assembly on a Microstructured Substrate

*Antoine Diguet, Maël Le Berre, Yong Chen, and Damien Baigl**

***B**y dragging a phospholipid solution on microstructured silicon surfaces, phospholipid molecules are selectively deposited inside the microstructures to get regular phospholipid multilayer patterns of controlled thickness over a large scale (~cm^2). By varying the dragging speed, the thickness of the patterns varies between 28 and 100 nm on average (7 to 25 bilayers). Electroswelling of phospholipid multilayer patterns leads to the formation of giant liposomes of controlled size and narrow size distributions.*

Keywords:
- capillary assembly
- multilayers
- patterning
- phospholipids
- supported membranes

1. Introduction

Patterning matter on a substrate in a controlled way is important for numerous fundamental and practical applications. Microcontact printing is probably the most widely used method for its versatility and compatibility with many materials (proteins, nanoparticles, DNA, bacteria, etc.).[1] However, although it allows for well-defined geometries with a high spatial resolution, the amount of deposited matter per unit area remains generally difficult to control except in some specific cases.[2] An interesting alternative to microcontact printing is capillary assembly on a microstructured substrate, which was originally proposed to organize colloids and nanoparticles.[3] In this paper, we describe the first capillary-assembly-based methodology to pattern organic molecules on a solid substrate with high resolution and control of the deposited amount. We applied this method to the large-scale patterning of phospholipid multilayers of controlled thickness and found that electroswelling of phospholipid multilayer patterns led to the formation of giant liposomes with narrow size distributions.

The controlled deposition of phospholipid films on a solid substrate is necessary for biological and biophysical investigations on supported membranes.[4] Various methods are now available to deposit one or a few (up to 5) bilayers on different surfaces in a controlled way, such as small unilamellar vesicles adsorption or Langmuir-Blodgett film deposition.[5] In contrast, much less efforts have been devoted to the deposition of thicker multilayered phospholipid films. Spin-coating is efficient but leads to poorly organized films.[6] Recently, we introduced the meniscus receding technique to spread very homogenous multilamellar phospholipid films with a controlled thickness (from 20 to 200 nm, i.e., 5 to 50 bilayers) with a bilayer resolution.[7]

On the other hand, the patterning of phospholipid films remains experimentally challenging. Various possibilities have been proposed for patterning supported bilayers[8] such as chemical[9] or photochemical[10] patterning, photolithography,[11] nanoshaving lithography,[12] soft lithography,[13] or Langmuir–Blodgett deposition.[14] Meniscus instabilities,[7] microcontact printing,[15] and dry lift off[16] have been proposed to pattern phospholipid multilayers but the organization and thickness of the deposited films are not controlled. To our knowledge, the only available method to pattern phospholipid multilayered films with a controlled thickness is dip-pen nanolithography.[17] Here we describe a simple methodology to generate phospholipid multilayer patterns with high fidelity and control of pattern thickness. It consists of dragging the meniscus of a phospholipid solution on a microstructured substrate with a solvent in partial wetting situation on the substrate material.

2. Results and Discussion

2.1. The Method

To generate the phospholipid patterns, a droplet of phospholipid solution (98 wt% of 1,2-dioleoyl-sn-glycero-3-phosphocholine (DOPC) and 2 wt% of 1-palmitoyl-2-[-6[{7-nitro-2-1,

[*] Dr. D. Baigl, A. Diguet, Dr. M. Le Berre, Prof. Y. Chen
Department of Chemistry
Ecole Normale Supérieure
24, rue Lhomond, F75005 Paris (France)
E-mail: damien.baigl@ens.fr

Supporting Information is available on the WWW under http://www.small-journal.com or from the author.

DOI: 10.1002/smll.200900368

3-benzoxadiazol-4-yl}amino]caproyl]-sn-glycero-3-phosphatidylcholine (NBD-PC, fluorescent probe) at 0.5 mg mL^{-1} in trichloroethylene) was dragged on a solid substrate at a constant speed v under controlled temperature (20 °C) using the set-up described in the Supporting Information (Figure S1). As substrates, we used microstructured silicon wafers with hexagonal arrays of holes (400-nm depth) and various diameters d (Figure 1a). To get phospholipid deposition only inside the holes, the solvent should be in a partial wetting situation on the planar parts of the substrate.[18] This condition was achieved by choosing trichloroethylene as a solvent and cleaning the microstructured silicon substrate in a piranha solution prior to phospholipid deposition. Thus, when the solution was dragged on the microstructured substrates, the contact line was moving on the planar parts of the substrate without phospholipid deposition but was pinned on the edges of the microstructures due to the steep increase of the contact angle, which resulted in the trapping of phospholipid solution in the substrate holes (Figures 1b and c and Supporting Information Movie 1). After solvent evaporation, a phospholipid multilayer film was selectively deposited in the microstructures. According to fluorescence microscopy observations, the patterns obtained by this technique are very regular (Figures 1d and e) over a large area (~cm^2). In contrast, using solvents with a very low contact angle for silicon (e.g., octane) or inappropriate cleaning of the silicon substrate led to non-specific deposition of phospholipid molecules (Supporting Information, Figure S2).

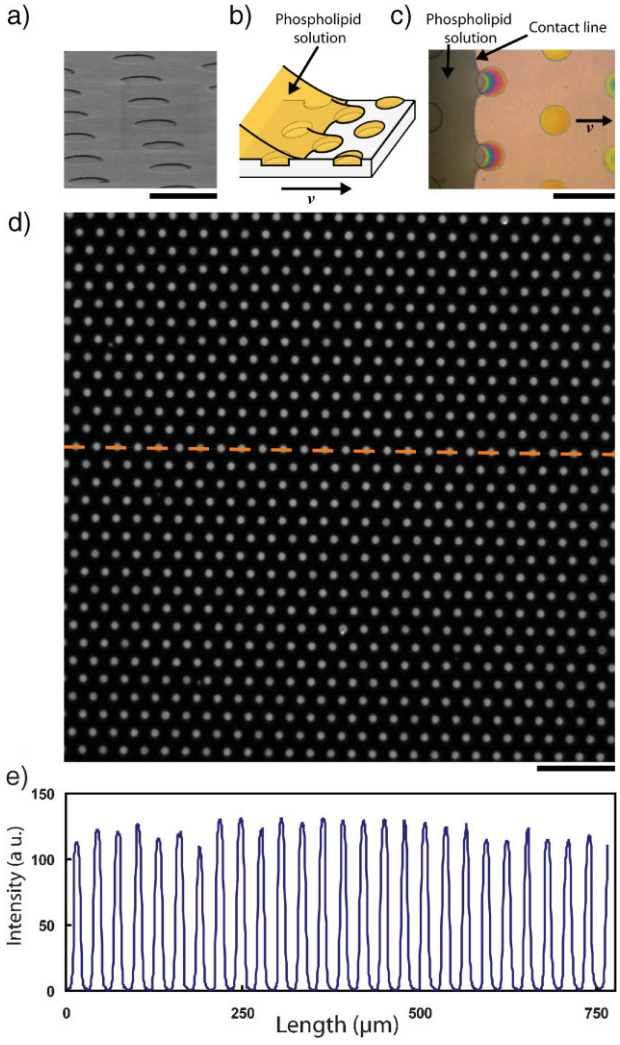

Figure 1. Regular phospholipid multilayer patterns are obtained by dragging a phospholipid solution on a microstructured silicon substrate (hexagonal array of holes, diameter d, depth 400 nm). a) SEM image of a microstructured silicon substrate ($d = 12$ μm). The scale bar is 20 μm. b) Principle of the deposition: the phospholipid solution, which is in a partial wetting situation on the planar parts of the substrate, is selectively deposited in the microstructures. c) Real-color image during the deposition of a phospholipid solution on a substrate ($d = 24$ μm). The arrow indicates the direction of the substrate translation. The scale bar is 50 μm. The corresponding movie (movie 1) is given in the Supporting Information. d) Fluorescence microscopy image of a phospholipid pattern obtained with $d = 12$ μm and a deposition speed $v = 25$ μm s^{-1}. The scale bar is 100 μm. e) Fluorescence intensity profile along the dashed line in (d). For all experiments, we used a phospholipid solution (98wt% DOPC, 2wt% NBD-PC) at 0.5 mg mL^{-1} in trichloroethylene.

2.2. Effect of Deposition Speed and Microstructure Size

Figure 2a shows the patterns and fluorescence intensity profiles obtained with three isomorphic microstructures (hexagonal arrays of holes with diameters d of 6, 12, and 24 μm; depth 400 nm) and various deposition speeds v (from 5 to 75 μm s^{-1}). First, regardless of d, the phospholipid patterns reproduce the substrate microstructures with high fidelity. Second, a strong effect of v is observed. Fluorescence intensity, which is a measure of the deposited phospholipid amount per hole, increases with a decrease in v. By using a calibration curve linking fluorescence intensity to the film thickness of flat films (Supporting Information Figure S3), we converted the fluorescence signal to the average film thickness in a hole. Figure 2b shows that the average film thickness in a hole is nearly independent of d and decreases as a function of v. When averaged for the three hole sizes, the thickness can be fitted by a linear behavior. It can be qualitatively explained as follows. The amount of liquid trapped in holes can be considered as independent of v, which is in agreement with observations of the meniscus moving on the microstructures. However, the accumulation of phospholipid near the contact line due to evaporation increases with a decrease in v, as has been shown for phospholipid droplets under evaporation on a flat substrate.[7] As a result, holes will be filled by similar amount of phospholipid solution but with a concentration that increases with a decrease in v. After evaporation, this will result in phospholipid film of larger thickness for smaller v regardless of d, which is in agreement with our experimental observations.

It is also interesting to note that the phospholipid organization inside the microholes depends on v and d. For $v \geq 40$ μm s^{-1}, phospholipid molecules organize into rings following the microstructure edges regardless of d. Since the solvent is in partial wetting conditions on the substrate, the droplet of phospholipid solution trapped in the microstructure takes a convex shape, and its evaporation is higher in its edge than in its centre. The resulting concentration gradient of phospholipid might induce a Marangoni flow that accumulates matter toward the edges of the microstructure.

NANO MICRO small

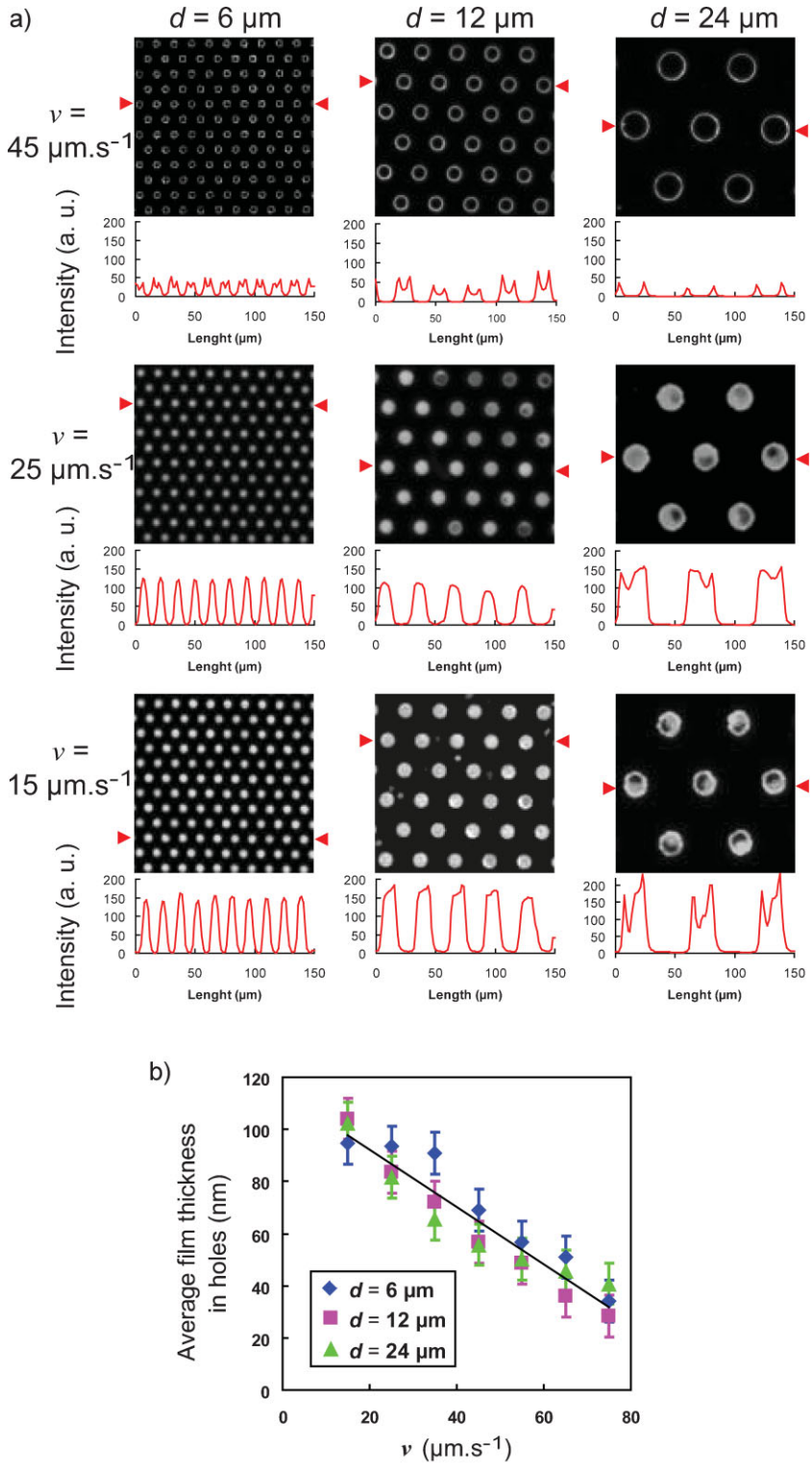

Figure 2. Microstructure hole diameter *d* and deposition speed *v* control the organization and thickness of deposited phospholipid patterns. a) Fluorescence microscopy images (top) and fluorescence intensity profiles between red arrows (bottom) of phospholipid patterns obtained for various values of *v* and *d*. Each image has a size of $150 \times 150\ \mu m^2$. b) Average film thickness of deposited phospholipid per hole as a function of *v* for various values of *d* (6, 12, and 24 µm). Each point represents the average measured on a surface $750 \times 750\ \mu m^2$. The conversion of the fluorescence into thickness was made using the calibration curve shown in Supporting Information, Figure S3). The black line is a linear fit of all data points (that is, regardless of *d*) and has the equation: $y = -1.1x + 114$ ($R^2 = 0.99$). For all experiments, we used a phospholipid solution (98wt% DOPC, 2wt% NBD-PC) at 0.5 mg mL^{-1} in trichloroethylene.

Since the amount of phospholipid per hole is small in the high-speed regime (Figure 2b), this flow can lead to a depletion of phospholipid from the center of the microstructure. For $v < 40\ \mu m\ s^{-1}$, holes are filled by the phospholipid and lead to very homogenous disks for $d = 6$ and $d = 12\ \mu m$. In this low-speed regime, the amount of phospholipid per hole is large and depletion from the microstructure center is probably hindered. However, for larger hole diameters ($d = 24\ \mu m$), some thickness heterogeneities are clearly visible in each hole. In this case, the fluorescence profiles indicate that the thickness of the phospholipid film tends to be smaller in the center of the microstructures, which can also be due to a Marangoni flow toward the microstructure edges. Since the amount of phospholipid is relatively large, only a partial depletion from the center is possible. It is important to note that the film thickness per hole shown in Figure 2b is calculated by assuming a homogenous disk shape in the hole. Therefore, in the case of heterogeneous disks (small speeds, large hole diameter) or rings (high speeds), it does not represent the actual thickness of the film in the hole but the amount of phospholipid deposited per surface unit. All these results show that our methodology allows very regular multilayer phospholipid patterns of various sizes and geometries to be obtained. Both thickness and phospholipid organization can be controlled by varying microstructure diameter or deposition speed.

2.3. Application to the Preparation of Giant Liposomes of Controlled Size Distribution

Finally, we used the generated phospholipid multilayer patterns for the preparation of giant liposomes of controlled size distribution. To this end, phospholipid multilayer patterns of DOPC were generated on microstructured silicon with a deposition speed of $15\ \mu m\ s^{-1}$ (approximately 20 bilayers). Then, they were electroswollen (2 V, 10 Hz, 4 h) in a sucrose solution (~0.1 M) by using indium tin oxide (ITO)-coated glass slide as a counter electrode, according to the so-called electroformation technique (Figure 3a). After electroformation, liposomes were extracted from the electroswelling compartment and introduced into a glucose solution (~0.1 M) having exactly the same osmolarity as that of the sucrose solution. After decantation by

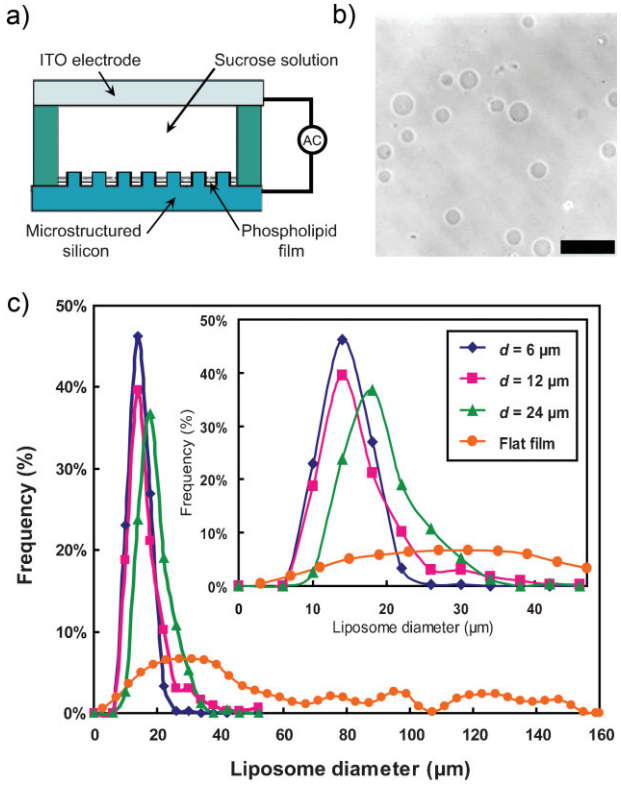

Figure 3. Electroswelling of phospholipid multilayer patterns leads to the formation of giant liposomes of controlled size distribution. a) Scheme of the electroswelling set-up. b) Typical phase-contrast microscopy image of liposomes collected after the electroswelling in sucrose of a DOPC multilayer patterns ($v = 15\ \mu m\ s^{-1}$, 20 bilayers in average, $d = 6\ \mu m$) and sedimentation in a glucose solution. The scale bar is 40 μm. c) Distribution of the liposome diameters obtained after electroformation from patterns of various diameters d. For comparison, the distribution obtained by electroswelling a manually deposited phospholipid film on a flat silicon substrate is also represented (orange symbols). The inset is a zoom for liposome diameters in the range 0–50 μm.

gravity (glucose is less dense than sucrose), giant liposomes were collected on a cover glass slide and observed by phase-contrast microscopy (Figure 3b). Figure 3c shows the size distribution of liposomes generated from patterns of various diameters compared to that obtained from a phospholipid film manually spread on a flat silicon wafer. Electroformation is the most robust and widely used technique to prepare a large number of unilamellar giant liposomes that can serve as primary artificial cell models[19] but it generally leads to a very broad distribution of the generated liposomes. A typical size distribution obtained by this technique (phospholipid film on a flat silicon wafer) is plotted in Figure 3c (orange symbols), showing a size variation in the range 1–150 μm with no clearly defined maximum. In contrast, the liposome size distributions obtained from the phospholipid multilayer patterns are very narrow with a very well defined maximum regardless of pattern size. Although the position of the maximum is not strongly correlated with the pattern size, the mean diameter of liposomes increases with an increase in pattern size. Our method thus provides a means to control the generation of giant liposomes of controlled size distribution by electroformation. Apart from electroformation,[15] microfluidic jetting[20] and double-emulsion templating[21] are the only available methods to get well-defined giant liposomes with narrow size distributions but they are more suitable for large liposome diameters (usually $\geq 100\ \mu m$).

3. Conclusions

We have shown how capillary assembly can be used to pattern molecules instead of nanoparticles or colloidal suspensions. Compared to microcontact printing, the main interest of this method is the possibility to control the number of molecules deposited per surface unit. Here, we applied this concept to generate for the first time phospholipid multilayer patterns of a controlled thickness. By dragging a phospholipid solution in partial wetting situation on microstructured silicon surfaces, centimeter-sized patterns were easily obtained with high fidelity. The amount and organization of deposited phospholipid molecules can be controlled by varying the deposition speed and microstructure size. The generated phospholipid patterns were used for the preparation of giant liposomes of controlled size with a narrow size distribution, which can be further used for investigations on artificial cell model systems. Regular phospholipid multilayer patterns can be of great interest for the development of novel biosensors or cell screening procedures. Not limited to phospholipid patterning, the method promises to be applicable for high-fidelity patterning of various synthetic or biological molecules, such as proteins, drugs, conductive polymers, or antibodies.

4. Experimental Section

Materials: [100] boron-doped Si wafers were from Siltronix. AZ 5214 photoresist was from Clariant (Wiesbaden, Germany). 1,2-dioleoyl-sn-glycero-3-phosphocholine (DOPC) and 1-palmitoyl-2-[-6[{7-nitro-2-1, 3-benzoxadiazol-4-yl}amino]caproyl]-sn-glycero-3-phosphatidylcholine (NBD-PC) phospholipids were from Avanti Polar Lipids (Alabaster, AL, USA). All other chemicals were from Sigma. Deionized water was used for all experiments.

Surface microstructuration: Silicon wafers were cleaned by air and isopropanol, then dried and rendered hydrophilic by air plasma treatment for 2 min at 500 mTorr (Plasma Cleaner, Harrick) and immediately exposed to a trimethylchlorosilane atmosphere. AZ 5214 photoresist was deposited on the Si wafer and spincoated (acceleration: 100 tr min^{-1} s^{-1}, speed: 500 tr min^{-1} for 5 s, then acceleration: 2000 tr min^{-1} s^{-1}, speed: 4000 tr min^{-1} for 30 s). The wafer was heated at 125 °C during 1 min and then irradiated by a UV lamp (30 mW cm^{-2}, Hamamatsu) through a mask for 2.6 s. After heating at 125 °C for 1 min, the wafer was irradiated under UV without mask for 1 min. After cooling, the wafer was immersed in a developer solvent (AZ 710 MIF, Clariant) and placed under a SF_6 reactive ion dry etching (30 mT, 10 W, 120 s with a Nextral NE100 RIE machine). The resist was dissolved in an acetone bath. The depth of holes was determined with Veeco Caliber atomic force microscopy (AFM) (Veeco Instruments, Santa

NANO MICRO small

Barbara, USA) in air at ambient temperature. Figure 1a was obtained with a Scanning Electron Microscope Hitachi 5-800 (Tokyo, Japan).

Phospholipid solution preparation: A chloroform solution containing a weight ratio of 98% DOPC and 2% NBD-PC was evaporated under vaccum for 20 min. The proper amount of thrichloroethylene was then added to obtain a 0.5 mg mL^{-1} concentration.

Phospholipid deposition: Phospholipid deposition was realized using a set-up described elsewhere [7]. Briefly, microstructured silicon substrates were cleaned by acetone prior to immersion in a piranha bath (1:3 vol H_2O_2/H_2SO_4 concentrated) and rinsing by water. Figure S1 shows the experimental setup for film deposition. The silicon substrate was mounted on a computer-controlled linear-translation stage (M-403.6 PD, PI) equipped with a thermoelectric module for temperature control. A 80 μL droplet of a phospholipid solution was held by a fixed poly(tetrafluoroethylene) (PTFE) slide (2-cm width) with a sharp end while the substrate was moved at constant speed v and temperature $T = 20\,^{\circ}C$. v was changed between 75 and 5 μm s^{-1} every 10 μm, or fixed at 15 μm s^{-1} to cover the microstructure on a surface of $1.6 \times 1.2\ cm^2$.

Observation of the deposition: A camera equipped with a long-distance objective was placed above the fixed PTFE slide. This allowed us to follow in real time the contact line moving on the microstructures during phospholipid deposition.

Characterization of the patterns: After solvent evaporation, phospholipid patterns were observed by fluorescence microscopy with an inverted microscope Axioobserver D1 (Carl Zeiss, Germany) with 10× and 20× objectives and a FITC filter. Pictures were acquired with a high-sensibility EM-CCD camera (Photonmax 512B, Princeton Scientific) and the acquisition software Metaview. The curve shown in Figure 2b was built as follows. First, homogenous films of various thicknesses were prepared by depositing a phospholipid solution on flat silicon wafers at various speed v [7]. The thickness of the films was measured by ellipsometry in air using a SentechSE400 apparatus. The light source was a helium-neon laser ($\lambda = 632.8$ nm), and the angle of incidence was set to 72°. The thickness was determined using a multilayer model and a refractive index of 1.45 for the phospholipid film. For each film, the measurement was repeated on 10 different locations. Then, the average fluorescence intensity was plotted as a function of the average thickness measured by ellipsometry to build the calibration curve shown in Figure S3. Finally, the average fluorescence intensity of phospholipid patterns on microstructured silicon was converted into the average thickness in microstructure holes by using the calibration curve shown in Figure S3 and by taking into account the surface ratio of the microstructures (microstructures represent 1/8 of the total surface for the three pattern sizes).

Electroswelling: The microstructured electrode was separated from a flat ITO electrode using a 4-mm silicon rubber spacer with a surface of 1 cm^2. The swelling solution contained 0.1 M sucrose and 4.6 mM NaN_3 in water. Electroswelling was realized with a sinusoidal AC field (2 V, 10 Hz) for 3 h. Liposome suspension was then extracted under low shear stress and mixed with 2 volumes of 0.1 M glucose solution containing 4.6 mM NaN_3 and previously adjusted to have the same osmolarity as that of the sucrose solution (104 mOsm L^{-1}). The liposomes mixed with the glucose solution were then collected by gravity on a microscope glass slide after 4 h of decantation.

Image analysis: Statistical data from phase contrast images (vesicles in glucose) were collected by manually measuring the size of each vesicle. Each distribution was established on approximately 300 measured vesicles.

Acknowledgements

This work was partially supported by the ICORP 2006 "Spatio-Temporal Order" project (Japan Science and Technology Agency), the Centre National de la Recherche Scientifique (CNRS), and the European Commission through project contract CP-FP 214566-2 (Nanoscales). M.L.B. received a grant from the EADS Foundation.

[1] A. Kumar, G. M. Whitesides, *Appl. Phys. Lett.* **1993**, *63*, 2002.
[2] a) J. Park, P. T. Hammond, *Adv. Mater.* **2004**, *16*, 530; b) M. C. Berg, S. Y. Yang, P. T. Hammond, M. F. Rubner, *Langmuir* **2004**, *20*, 1362.
[3] a) Y. Yin, Y. Lu, B. Gates, Y. Xia, *J. Am. Chem. Soc.* **2001**, *123*, 8718-L 8729; b) Y. Cui, M. T. Björk, J. A. Liddle, C. Sönnichsen, B. Boussert, A. P. Alivisatos, *Nano Lett.* **2004**, *4*, 1093; c) T. Kraus, L. Malaquin, E. Delamarche, H. Schmid, N. D. Spencer, H. Wolf, *Adv. Mat.* **2005**, *17*, 2438; d) Y. K. Koh, C. C. Wong, *Langmuir* **2006**, *22*, 897; e) Z. Yuan, D. B. Burckel, P. Atanassov, H. Fan, *J. Mater. Chem.* **2006**, *16*, 4637; f) T. Kraus, L. Malaquin, H. Schmid, W. Riess, N. D. Spencer, H. Wolf, *Nature Nanotech.* **2007**, *2*, 570; g) L. Malaquin, T. Kraus, H. Schmid, E. Delamarche, H. Wolf, *Langmuir* **2007**, *23*, 11513.
[4] E. Sackmann, *Science* **1996**, *271*, 43.
[5] a) G. Roberts, *Langmuir-Blodgett Films; Plenum Press* **1990**; b) B. L. Stottrup, S. L. Veatch, *Biophysical J.* **2004**, *86*, 2942; c) Y. Ohta, S. Yokoyama, H. Sakai, M. Abea, *Colloids Surf. B: Biointerfaces* **2004**, *34*, 147.
[6] D. J. Estes, M. Mayer, *Colloids Surf. B: Biointerfaces* **2005**, *42*, 115.
[7] M. Le Berre, Y. Chen, D. Baigl, *Langmuir* **2009**, *25*, 2554.
[8] a) M. Tanaka, E. Sackmann, *Nature* **2005**, *437*, 656; b) J. T. Groves, S. G. Boxer, *Acc. Chem. Res.* **2002**, *35*, 149.
[9] J. T. Groves, N. Ulman, S. G. Boxer, *Science* **1997**, *275*, 651.
[10] C. K. Yee, M. L. Amweg, A. N. Parikh, *J. Am. Chem. Soc.* **2004**, *126*, 13962.
[11] C. K. Yee, M. L. Amweg, A. N. Parikh, *Adv. Mater.* **2004**, *16*, 1184.
[12] J. Shi, J. Chen, P. S. Cremer, *J. Am. Chem. Soc.* **2008**, *130*, 2718.
[13] P. Kim, S. E. Lee, H. S. Jung, H. Y. Lee, T. Kawai, K. Y. Suh, *Lab Chip* **2006**, *6*, 54.
[14] a) M. Gleiche, L. F. Chi, H. Fuchs, *Nature* **2000**, *403*, 173; b) X. Chen, M. Hirtz, H. Fuchs, L. Chi, *Langmuir* **2007**, *23*, 2280.
[15] a) P. Taylor, C. Xu, P. D. I. Fletcher, V. N. Paunov, *Phys. Chem. Chem. Phys.* **2003**, *5*, 4918; b) P. Taylor, C. Xu, P. D. I. Fletcher, V. N. Paunov, *Chem Commun.* **2003**, 1732; c) M. Le Berre, M. A. Guedeau-Boudeville, Y. Chen, D. Baigl, *Proc. microTAS* **2006**, 1399.
[16] K. Kuribayashi, S. Takeuchi, *Proc. microTAS* **2005**, 1455.
[17] a) S. Lenhert, P. Sun, Y. Wang, H. Fuchs, C. A. Mirkin, *Small* **2006**, *3*, 71; b) R. D. Piner, J. Zhu, F. Xu, S. Hong, C. A. Mirkin, *Science* **1999**, *283*, 661.
[18] P. M. Moran, F. F. Lange, *Appl. Phys. Lett.* **1999**, *74*, 1332.

[19] a) M. I. Angelova, D. S. Dimitrov, *Faraday Discuss. Chem. Soc.* **1986**, *81*, 303; b) F. M. Menger, M. E. Chlebowski, A. L. Galloway, H. Lu, V. A. Seredyuk, J. L. Sorrells, H. Zhang, *Langmuir* **2005**, *21*, 10336; c) R. Dimova, S. Aranda, N. Bezlyepkina, V. Nikolov, K. A. Riske, R. Lipowsky, *J. Phys.: Condens. Matter* **2006**, *18*, 1151; d) Y. Okumura, H. Zhang, T. Sugiyama, Y. Iwata, *J. Am. Chem. Soc.* **2007**, *129*, 1490; e) M. Le Berre, A. Yamada, L. Reck, Y. Chen, D. Baigl, *Langmuir* **2008**, *24*, 2643.

[20] a) K. Funakoshi, H. Suzuki, S. Takeuchi, *J. Am. Chem. Soc.* **2007**, *129*, 12608; b) J. C. Stachowiak, D. L. Richmond, T. H. Li, A. P. Liu, S. H. Parekh, D. A. Fletcher, *Proc. Natl. Acad. Sci. USA* **2008**, *105*, 4697.

[21] H. C. Shum, D. Lee, I. Yoon, T. Kodger, D. A. Weitz, *Langmuir* **2008**, *24*, 7651.

Received: March 2, 2009
Revised: April 15, 2009
Published online: May 22, 2009